

INSTITUTE OF GAS TECHNOLOGY
IGT CENTER
CHICAGO, ILLINOIS 60616

PREPARATION OF A
COAL CONVERSION SYSTEMS
TECHNICAL DATA BOOK
ERDA Contract No. E(49-18)-1730
Report No. 5
March 1975

Project 8964 Status Report
for
ENERGY RESEARCH AND DEVELOPMENT ADMINISTRATION



INSTITUTE OF GAS TECHNOLOGY - 117 CENTER - CHICAGO 60616

Project Status Report
for

ENERGY RESEARCH AND DEVELOPMENT ADMINISTRATION

Report for
March 1975

Project Title : Preparation of a Coal Conversion Systems Technical
Data Book

ERDA Contract No. E(49-18)-1730

I. Project Objective

The objective of this work is to provide a single, comprehensive source of data on coal conversion systems. This compilation shall be entitled The Coal Conversion Systems Technical Data Book and shall provide up-to-date data and information for the research, development, design, engineering, and construction of coal conversion processes and/or plants. Other concurrent objectives are to identify those areas where data are required and to suggest research programs that will provide the required data.

II. Summary

Liquefaction

Product data for coal liquefaction processes are presented in a simpler form, which is much more suited for correlating the effects of coal type and operating parameters, by using the normal probability density function -

$$f_n(X) = \frac{1}{\sigma\sqrt{2\pi}} \exp \left[-\frac{(X-\mu)^2}{2\sigma^2} \right]$$

The entire yield structure of a given liquefaction operation up to coke can be expressed in terms of only two parameters, σ and μ . It should be possible to correlate these parameters with coal and solvent types as well as with operating conditions to give a comprehensive picture of the coal liquefaction process.

BLANK PAGE

Gasification

The results of the computations for steam-oxygen gasification of char at 15-atm pressure and four reaction temperatures are presented. These computations are also based on the base-case assumptions of completely backmixed gas and solid flow in the fluid bed and the unconverted, but completely devolatilized, feed char ($X_0 = 0.0$).

A correction chart is presented to calculate the residence time required for the same amount of carbon gasification (conversion) in the reactor when the feed char is partially gasified ($X_0 > 0.0$).

Another correction chart gives a multiplication factor to convert the solids residence time obtained for the "solids backmixed model" to the case where solids are in plug flow. Gas flow in both cases is assumed to be backmixed.

Fluidization

A correlation is proposed for the calculation of the minimum fluidization velocity required for coal and other related materials used in the conversion processes. This correlation fits the available data better than any other correlation investigated in this study.

Various correlations, available in the literature, for estimating the bed expansions are being evaluated. A comparison of some of these with the available data is also presented.

Combustion

A model is being developed to describe the sulfur removal from fluidized-bed combustors.

Coal, Char, and Oil Shale Properties

A list of large coal deposits (~150 million tons recoverable) is being prepared. This will cover both the underground mining and the strippable reserves.

A preliminary review of information on specific heats of coal, char, and ash is presented.

Notice to Readers of Open File

Any comments about the material presented in this report or suggestions about the format and the content of the data book as well as the priorities of the needed data are most welcome. Please direct any communications to Mr. Bipin Almaula of ERDA (202/634-6643) or to Dr. Al Talwalkar of the Institute of Gas Technology (312/225-9600, Ext. 869).

III. Work Accomplished

A. LIQUEFACTION

1. Correlation of Coal Liquefaction Yield Structure

Yield data for coal liquefaction processes are generally presented in the form of C₁-C₃ gas yields followed by yields and product properties of cuts of oil product boiling at various temperature ranges. It is possible to express all these data in a considerably simpler form much more suited to correlation of effects of coal type and operating parameters by transforming the yield data using the normal probability density function:

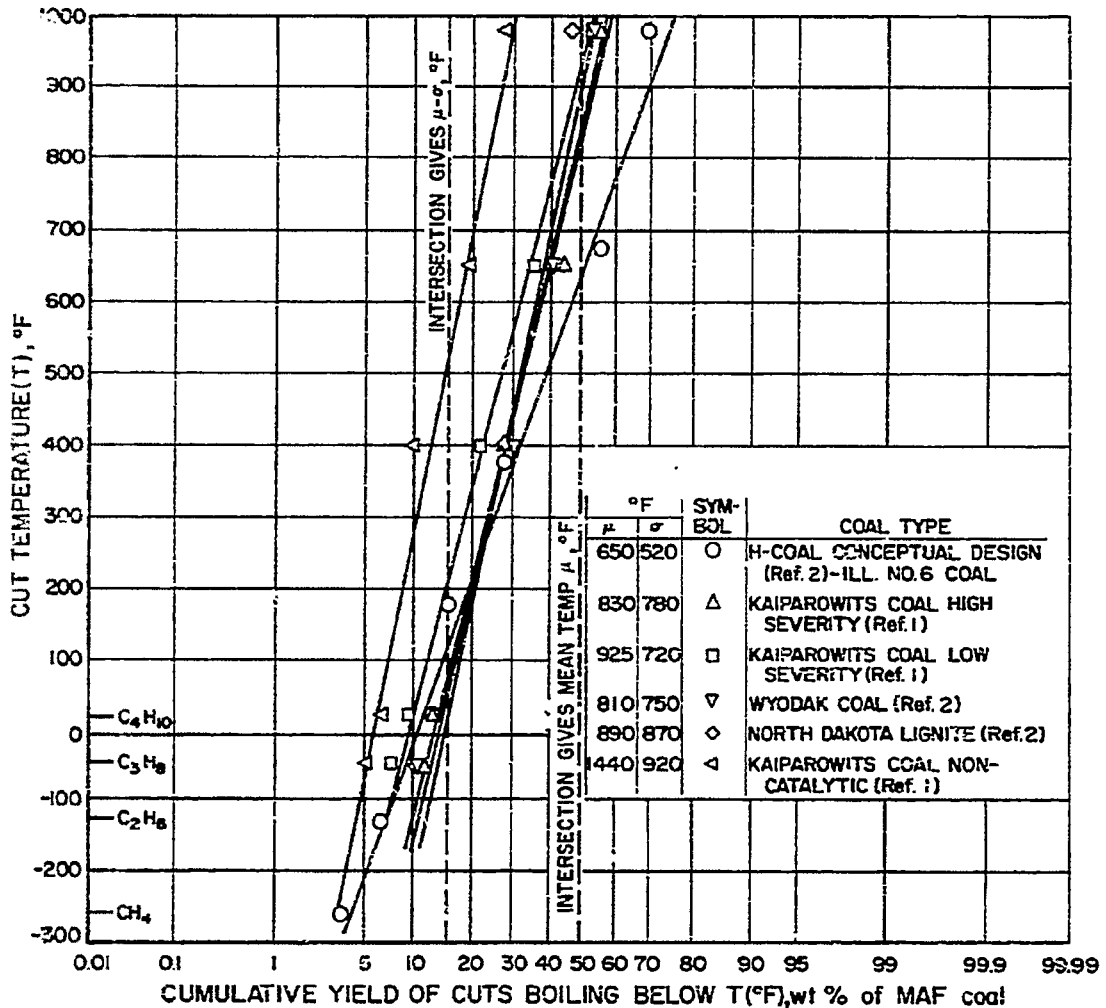
$$f_n(X) = \frac{1}{\sigma\sqrt{2\pi}} \exp \left[-\frac{(X-\mu)^2}{2\sigma^2} \right] \quad (1)$$

The entire yield structure of a given liquefaction operation up to coke can be expressed in terms of only two parameters, σ and μ . It should be possible to correlate these parameters with reactant properties and kinetic data to give a much more complete quantitative picture of coal liquefaction than has been available before.

It is known³ that distillation curves of most crude oils have a characteristic S-shape that indicates a relatively large amount of oil distilled near the average or mid-boiling point with less oil being distilled at lower or higher temperatures. These distillation curves are, in fact, almost normally distributed with respect to temperature and show as straight lines plotted on arithmetic probability paper. Experimental data for the H-COAL operation^{1,2} exhibit the same type of behavior. Figure 1 shows experimental data for several H-COAL operations and for a blank run made without catalyst.



ERDA	_____
PAGE	_____
REVISION No.	_____
DATE	_____



B75030587

Figure 1. PRODUCT DISTRIBUTION CURVES FOR H-COAL OPERATION

PRELIMINARY
FOR REVIEW ONLY

The straight lines plotted on Figure 1 indicate that the yield structure can be expressed as -

$$Y = \frac{\text{Cumulative Yield Boiling Below } T \text{ (}^\circ\text{F) Based on Weight Fraction of MAF Coal Feed}}{\int_{-\infty}^T \frac{1}{\sigma\sqrt{2\pi}} \exp \left[-\frac{(T-\mu)^2}{2\sigma^2} \right] dT} \quad (2)$$

$$Y = N \left(\frac{T-\mu}{\sigma} \right) \quad (3)$$

Equation 2 cannot be expressed in terms of elementary functions, but numerous tabulations of the function N (the normal distribution with mean $\mu = 0$ and variance $\sigma^2 = 1$) are available.

The parameters μ and σ for a given run can be determined directly from Figure 1 by recalling that -

$$\frac{T-\mu}{\sigma} = 0 \text{ at } Y = 0.50 = N(0) \quad (4)$$

$$\frac{T-\mu}{\sigma} = -1 \text{ at } Y = 0.159 = N(-1) \quad (5)$$

The temperatures at $Y = 0.50$ and $Y = 0.159$ are read from Figure 1 and values substituted into Equations 4 and 5, respectively. For the H-COAL conceptual design, $\mu = 650^\circ\text{F}$ and $\sigma = 520^\circ\text{F}$. Given μ and σ , it is a simple matter to construct the product distribution curve. The curve is merely a straight line through $(T = \mu, Y = 0.50)$ and $(T = \mu - \sigma, Y = 0.159)$.

Alternatively, μ and σ can be determined numerically by determining X_i for each cut point observation from the equation -

$$Y_i = N(X_i) \quad (6)$$

and fitting the equation

$$T = \mu + X\sigma \quad (7)$$

to the resulting pairs of (T_i, X_i) data using the method of least squares. Results of this approach are shown in Figure 2. This method gave $\mu = 653^\circ\text{F}$ and $\sigma = 520^\circ\text{F}$, very close to the values determined graphically. The standard



ERDA	_____
PAGE	_____
REVISION No.	_____
DATE	_____

RUN REG*

STRAIGHT LINE FIT FOR TWO VARIABLES 24-MAR-75

DO YOU WISH DETAILED INSTRUCTIONS? NO

WILL INPUT BE FROM "FILE" OR "KEY"? FILE

GIVE INPUT FILE NAME-- LIQF

DATA FILE INDICATES 2 VARIABLES.

GIVE SUBSCRIPT OF VARIABLE TO BE CALLED X: 2

GIVE SUBSCRIPT OF VARIABLE TO BE CALLED Y: 1

DO YOU WANT TO FORCE THE EQUATION THROUGH A CERTAIN POINT? NO

$$Y = 552.8016662 + 520.2541198 X$$

**PRELIMINARY
FOR REVIEW ONLY**

53.38812303 STANDARD ERROR ABOUT THE LINE

0.9932

LINEAR CORRELATION COEFFICIENT R

THIS IS SIGNIFICANTLY DIFFERENT FROM ZERO AT
THE 99.9% LEVEL, USING FISHER'S Z TEST

2.4469

TWO-SIDED T(.950, 6.DF)

95.0% CONFIDENCE LIMITS ON THE INTERCEPT 6.5280E+02 ARE
534.6365203 AND 720.9668121

95.0% CONFIDENCE LIMITS ON THE SLOPE OF 5.2025E+02 ARE
459.3515434 AND 581.1567001

DO YOU WANT PREDICTED VALUES AND CONFIDENCE LIMITS PRINTED? YES

X	LOWER 95.0% CONFIDENCE LIMITS ON MEAN VALUE	MEAN VALUE	UPPER 95.0% CONFIDENCE LIMITS ON MEAN VALUE
-1.839	-381.0579299	-303.8598175	-226.6617069
-1.445	-158.7101249	-98.96053741	-39.25095081
-1.051	57.66862392	105.8967503	154.1282776
-0.657	263.5010490	310.7780303	358.0550117
-0.264	458.2593460	515.6573181	573.0552902
0.130	646.3450393	720.5365982	794.7281646
0.524	831.2633743	925.4158859	1019.568397

Figure 2. COMPUTER DETERMINATION OF μ AND σ FOR H-COAL
CONCEPTUAL DESIGN USING METHOD OF LEAST SQUARES

error of estimate, which is an indication of the goodness of fit of Equation 7 to the original data, was 53°F. This means that there is a probability of about 70% that, given Y, Equation 2 would predict T within $\pm 53^\circ\text{F}$. This is equivalent to saying that, for the region near 650°F, there is a 70% probability that Equation 7 would predict yields within 3% of the true value. (For example, at 650°F, the yield would be between 47% and 53%.) This is certainly well within the original limits of experimental error, since material balance closures were in the 95% to 105% range and occasionally were as low as 85% for this work.^{1, 2}

In addition to the numerical representation of Equation 1, this method of representing liquefaction data as in Figure 1 provides a graphical expression of several important facts about a given run. The mean temperature, μ , provides a quick indication of the overall product weight. The "spread temperature," σ , provides an indication of how concentrated the hydrocarbon product distribution curve is about the mean temperature, μ . A flat curve in Figure 1 will have a low value of σ , indicating a narrow product distribution whereas a wide product distribution will give a larger value of σ and a steeper curve in Figure 1.

Future data book work on coal liquefaction will include —

- a. Collecting available data from the literature we have surveyed and from our contacts with other researchers and determining characteristic parameters for these data
- b. Checking functions related to Equation 1 such as the log-normal or Poisson distributions to see if the fit to experimental data can be improved
- c. Attempting to include residual oil and coke yields in the correlation by statistically determining "characteristic cut temperatures" for these materials
- d. Correlating other oil properties such as sulfur content with cut weight (boiling point). Previous IGT work in this area with very heavy crude oils was quite successful.
- e. Relating the two parameters, μ and σ , to operating conditions and reactant properties
- f. Expressing available kinetic data in terms of our new product distribution model
- g. Indicating areas where further research would be most beneficial.

2. Nomenclature

- f_n = normal probability density function
 Y = cumulative yield of hydrocarbon gas and liquid products of liquefaction expressed as weight fraction of MAF Coal Feed
 $N(x)$ = normal probability distribution ($\mu = 0, \sigma^2 = 1$)
 μ = "mean temperature," °F
 σ = "spread temperature," °F
 T = upper cut temperature, °F
 X = defined by Equation 6

3. Example

Correlation of experimental data has shown that a particular process operating on a specific coal gives a yield structure with mean temperature $\mu = 800^\circ\text{F}$ and a spread temperature $\sigma = 700^\circ\text{F}$. Determine the yield of C_3 - 180°F oil that can be expected.

The temperature range in question is $+20^\circ\text{F}$ to 180°F , since a mixture of iso- and n-butane could be expected to boil at about 20°F . Recall that if a variable T that is normally distributed with mean μ and variance σ^2 , the variable —

$$X = \frac{T - \mu}{\sigma}$$

will be normally distributed with mean = 0 and variance = 1.

$$X_1 = \frac{20 - 800}{700} = -1.1143$$

$$N(-1.1143) = 0.1326 \quad [\text{From table of normal distribution (Equation 2)}]$$

$$X_2 = \frac{180 - 800}{700} = -0.8857$$

$$N(-0.8857) = 0.1879$$

$$N(X_2) - N(X_1) = 0.0553$$

The yield of $C_5-180^\circ F$ naphtha would be about 5.53% of the MAF coal fed.

4. References Cited

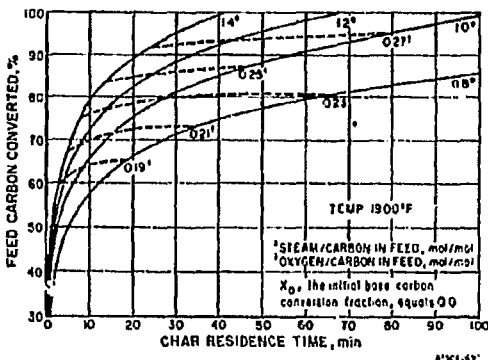
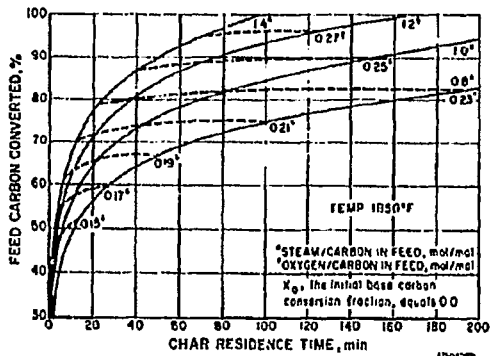
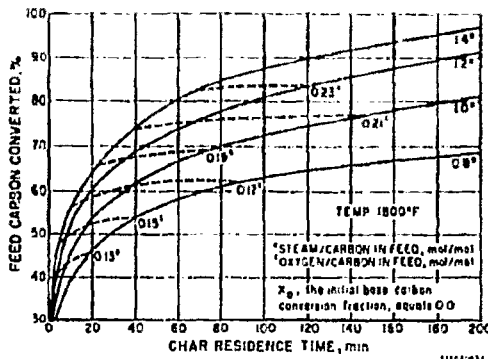
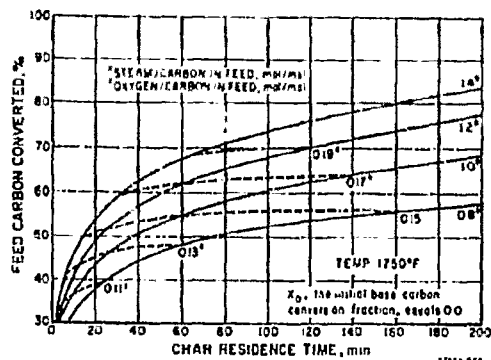
1. Hydrocarbon Research, "Liquefaction of Kaiparowits Coal," EPRI 123-2, Palo Alto, Calif.: Electric Power Research Institute, October 1974.
2. Hydrocarbon Research, "Project H-COAL Report on Process Development," OCR R&D Rep. No. 26, Washington, D. C.: Office of Coal Research, n. d.
3. Nelson, W. L., "Does Crude Boil at $1400^\circ F$?" Oil Gas J. 67, 125 (1968) March 25.

B. GASIFICATION

1. Steam-Oxygen Gasification of Char at 15 atm

Last month, we described the steam-oxygen-char gasification system for operation at 70-atm pressure and four gasification temperatures. This month, similar curves to determine the solids residence time and product gas compositions are given for operation at 15-atm pressure. These charts are also for the base-case conditions - fluidized-bed model with both gases and solids in backmixed flow and base carbon conversion fraction in the feed char, $X_0 = 0$.

For a given gasification temperature and 15-atm pressure, Figure 3 presents curves that give the char residence time required to achieve a specified feed carbon conversion at different steam feeds to the gasifier. The charts also show the amount of oxygen that is required in the feed to maintain adiabatic operation at any operating condition. The steam and the oxygen feeds have been normalized with respect to carbon in the char feed to make the charts more generally applicable. Normally, to achieve 100% feed carbon conversion, the solids residence time required would be infinite. However, because part of the char feed is combusted with oxygen to supply heat to the system, it is possible to achieve 100% conversion and yet have a finite solids residence time.



**PRELIMINARY
FOR REVIEW ONLY**



ERDA	_____
PAGE	_____
REVISION NO.	_____
DATE	_____

Figure 3. STEAM-OXYGEN GASIFICATION OF DEVOLATILIZED IRELAND MINE BITUMINOUS CHAR AT VARIOUS TEMPERATURES AND AT 15-atm PRESSURE

a. Gas Composition Versus Carbon Conversion Curves

Once the gasifier has been sized for a given carbon conversion, feed steam, and operating temperature, it is necessary to know the quantity and the composition of the product gas. The curves in Figures 4, 5, 6, and 7 show the total number of moles of product gas as well as the composition of the product gas as a function of feed carbon conversion for a given steam feed and operating temperature. Once again, for a generalized application, the curves have been normalized with respect to the carbon in the char feed to the gasifier. Note that this month the gas composition curves are not presented on a cumulative percentage basis as in the last report.

2. Adjustments for Variations From the Base Case

a. Partially Gasified Char Feed, $X_0 > 0$

In the charts presented in last month's report, the feed to the steam-oxygen gasifier was devolatilized char from which no base carbon had been gasified; that is, X_0 , the base carbon conversion fraction in the feed char, equals 0. In some applications, however, it would be desirable to feed char from which some of the base carbon had been gasified. The kinetic rate equation presented in last month's report provides a basis for adjusting the required solids residence times for specified conditions of operation at $X_0 = 0$, to describe the required solids residence times where $X_0 > 0$. For conditions where the absolute amount of carbon gasified is unchanged and all other operating conditions are the same, the difference in residence times for the case where $X_0 = 0$ and $X_0 > 0$ is shown in Figure 8. This figure presents a chart that gives the residence time factor -

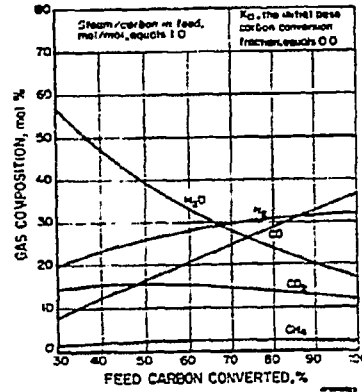
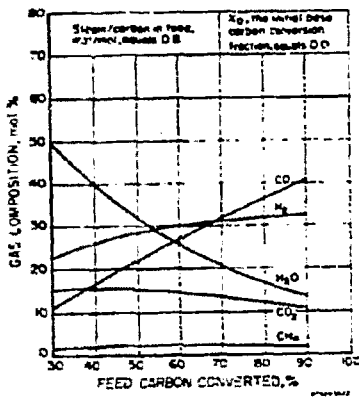
$$M = \frac{\text{residence time for } X_0 > 0}{\text{residence time for } X_0 = 0}$$

for different initial base carbon conversion fractions as a function of the corrected carbon conversion fraction. The corrected carbon conversion fraction, Y , is defined as follows:

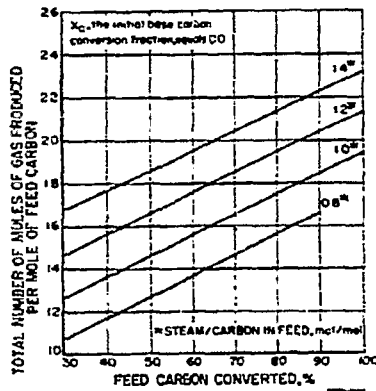
$$Y = \left(\frac{\text{total carbon gasified in gasifier}}{\text{carbon fed to gasifier}} \right) - \left(\frac{\text{oxygen fed to gasifier}}{\text{carbon fed to gasifier}} \right), \frac{\text{mol}}{\text{mol}}$$



ERDA	_____
PAGE	_____
REVISION No.	_____
DATE	_____



**PRELIMINARY
FOR REVIEW ONLY**



**PRELIMINARY
FOR REVIEW ONLY**

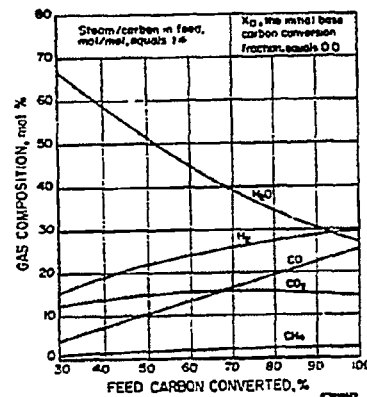
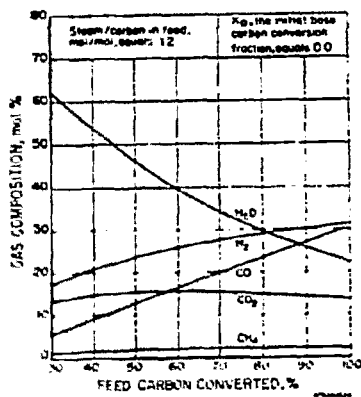
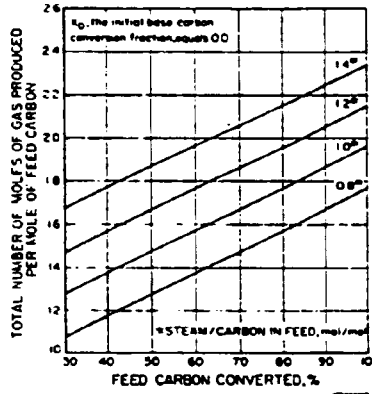
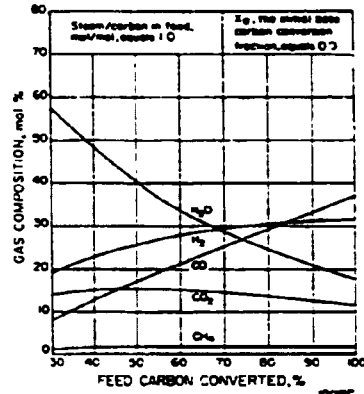
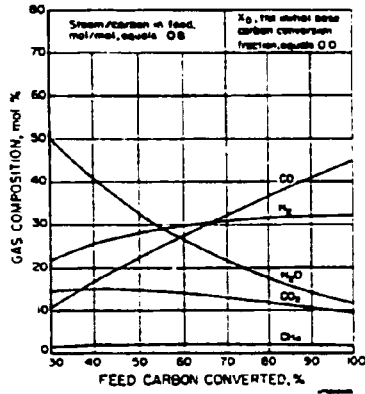


Figure 4. STEAM-OXYGEN GASIFICATION - PRODUCT GAS COMPOSITIONS
(Temperature = 1750°F; Pressure = 15 atm)



ERDA	_____
PAGE	_____
REVISION No.	_____
DATE	_____



PRELIMINARY
FOR REVIEW ONLY

PRELIMINARY
FOR REVIEW ONLY

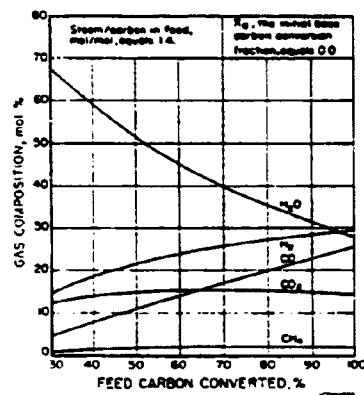
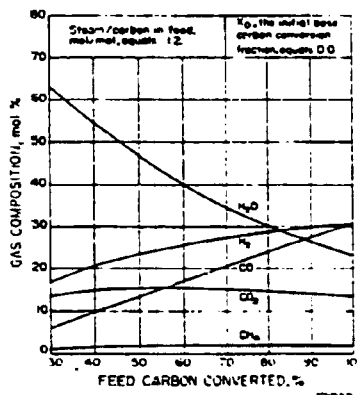
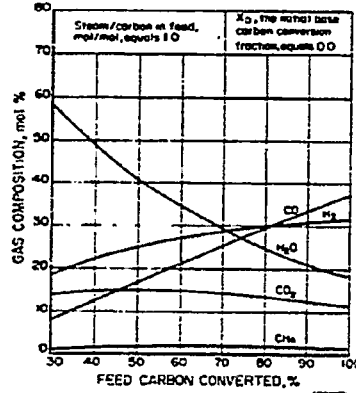
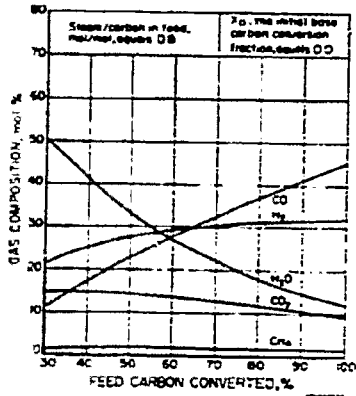


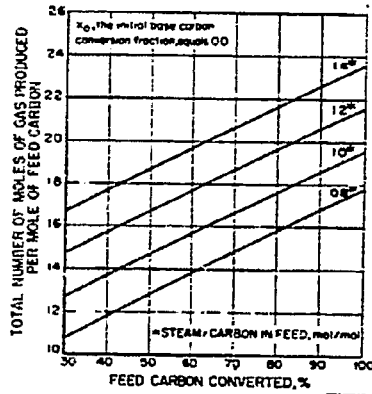
Figure 5. STEAM-OXYGEN GASIFICATION - PRODUCT GAS COMPOSITIONS (Temperature = 1800°F; Pressure = 15 atm)



ERDA	_____
PAGE	_____
REVISION No.	_____
DATE	_____



**PRELIMINARY
FOR REVIEW ONLY**



**PRELIMINARY
FOR REVIEW ONLY**

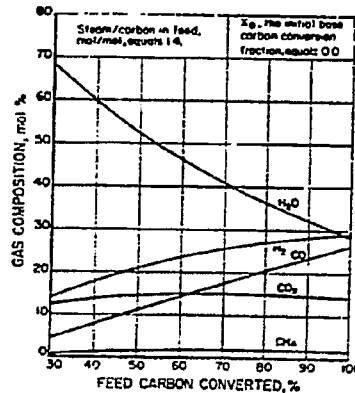
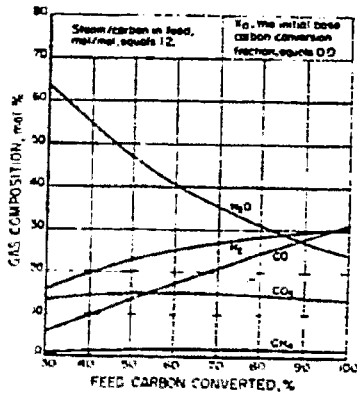
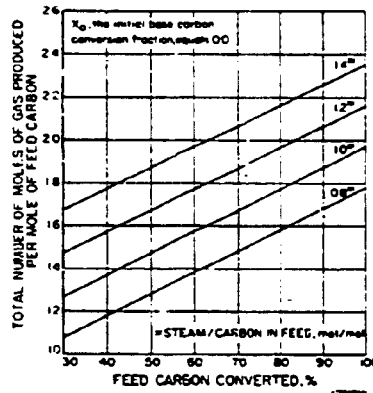
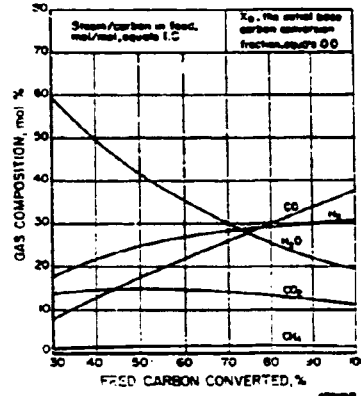
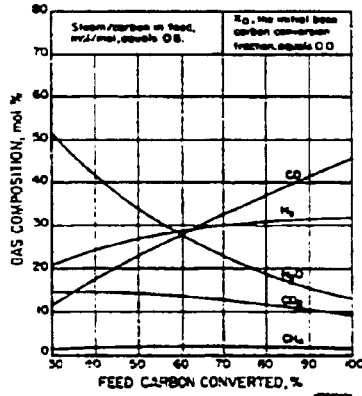


Figure 6. STEAM-OXYGEN GASIFICATION -- PRODUCT GAS COMPOSITIONS (Temperature = 1850°F; Pressure = 15 atm)



ERDA	_____
PAGE	_____
REVISION No.	_____
DATE	_____



**PRELIMINARY
FOR REVIEW ONLY**

**PRELIMINARY
FOR REVIEW ONLY**

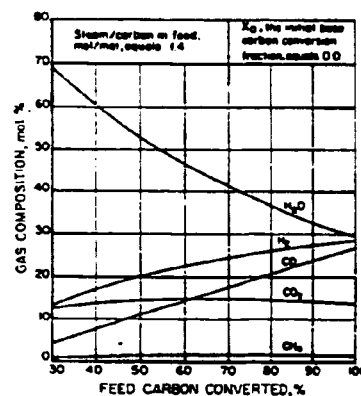
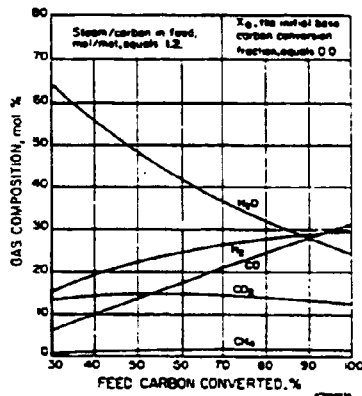


Figure 7. STEAM-OXYGEN GASIFICATION - PRODUCT GAS COMPOSITIONS (Temperature = 1900°F; Pressure = 15 atm)



ERDA	_____
PAGE	_____
REVISION No.	_____
DATE	_____

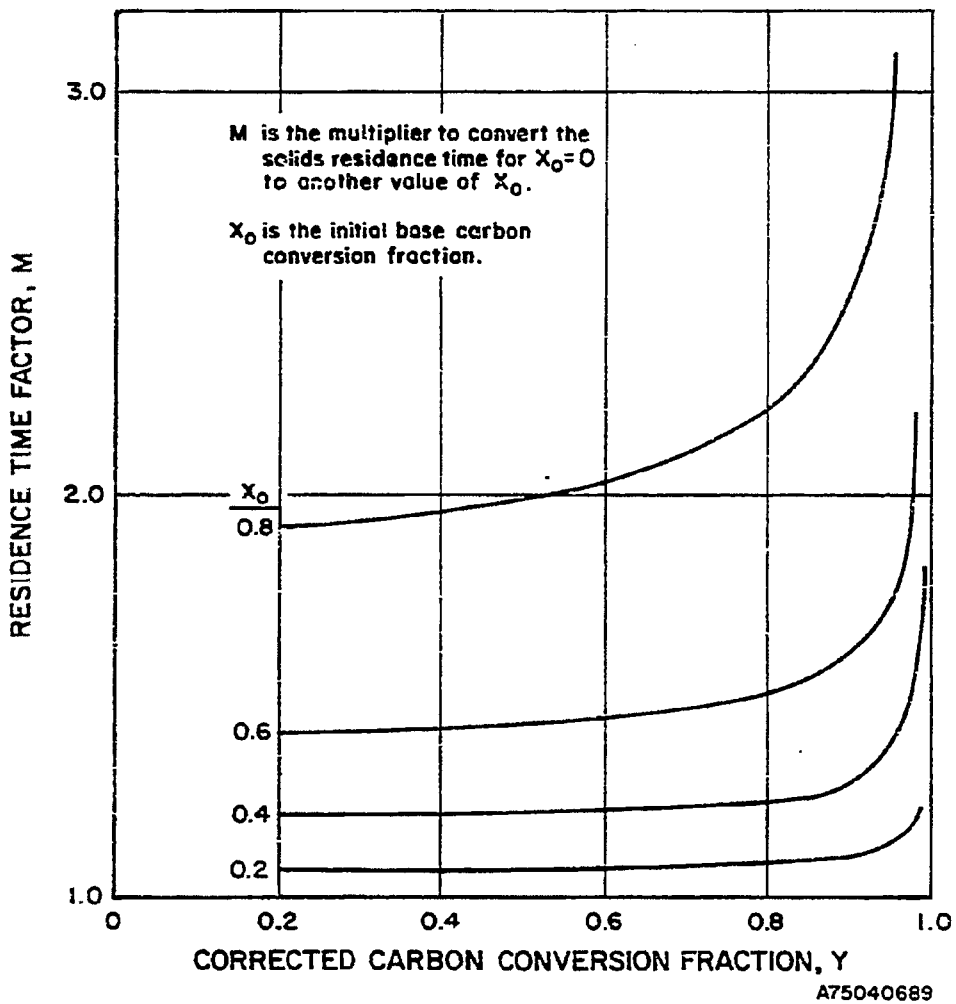


Figure 8. CONVERSION FACTOR FOR PARTIALLY GASIFIED CHAR FEED

PRELIMINARY
FOR REVIEW ONLY

Using charts presented in last month's report, the residence time for $X_0 = 0$ is read off for a desired feed carbon conversion:

$$\frac{\text{total carbon gasified in gasifier}}{\text{carbon feed to gasifier}}$$

Also, from the same chart, the corrected carbon conversion fraction, Y , is calculated. The residence time is then multiplied by M , which is obtained from Figure 8 at the specified values of Y and X_0 . The gas composition and other information do not require any adjustment because the absolute carbon gasified is unchanged.

b. Fluidized-Bed Model: Gas Backmixed and Solids Plug Flow

In the design charts presented in last month's report, the ideal fluidized model assumed that both the gas and the solids were completely backmixed in the bed. This gas-solids contacting model along with detailed kinetic correlations describing local reaction rates have been used at IGT to predict, with reasonable accuracy, the performance of 4-inch and 6-inch fluidized-bed steam-oxygen gasification reactors. However, under certain circumstances, it would be of interest to characterize behavior in a fluidized bed in which the gas is backmixed but the solids are in plug flow.

The main difference between the two types of gas-solids contacting models relates to the solids residence time required in the fluidized bed to achieve a specified feed carbon conversion for defined temperatures, pressures, and input flow rates.

This difference results because, for a solids plug-flow system, all solid particles have the same residence time, whereas for an ideally backmixed solids system, solids exiting from the fluid bed have a distribution of residence times. Because of the empirical form of the correlation describing the overall rate of carbon gasification (Equation 3 in last month's report), that is -

$$\frac{dX}{dt} = f_L k_T (1 - X)^{2/3} \exp(-\alpha X^2)$$

the average solids residence time required to achieve a specific amount of carbon conversion under gaseous environmental conditions is different for solids in plug flow than for backmixed solids, with the time for backmixed solids generally being greater.

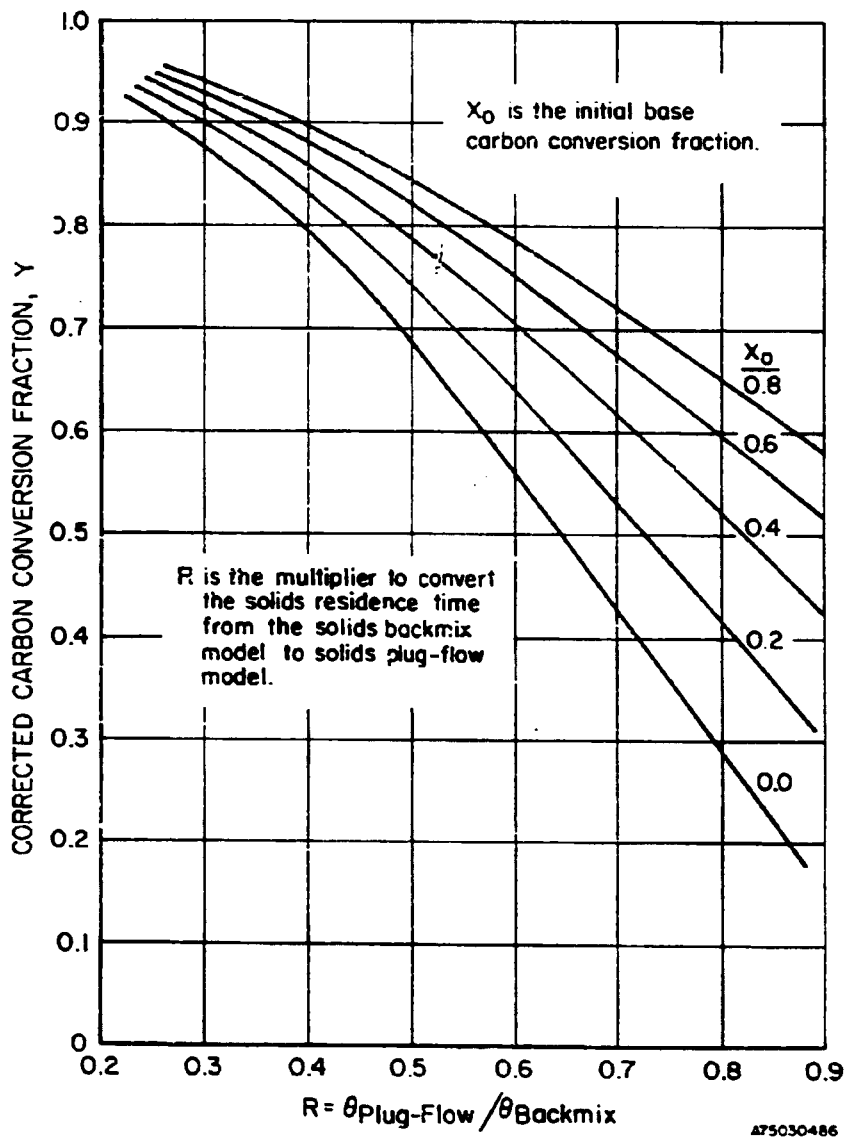
All the information presented in last month's report applicable to the solids-backmixed model can be used for the plug-flow model with the exception of reported solids residence times. The residence times required for plug-flow solids at specified operating conditions, however, can be calculated from the corresponding residence time based on the backmixed solids model, and charts can be prepared to define the necessary adjustments.

Figure 9 presents a conversion factor, R (the ratio of residence time for plug flow to the residence time for backmix), as a function of corrected carbon conversion fraction, Y , and initial base carbon conversion fraction, X_0 , defined in the preceding section.

For a given total feed carbon conversion fraction, the backmix model residence time can be obtained from Figure 3. Then a corrected carbon conversion fraction can be calculated from the oxygen consumption given in Figure 3. Using Figure 9, the conversion factor, R , is obtained for the corrected final carbon conversion fraction, Y , at a specified value of X_0 . The plug-flow model residence time is calculated by multiplying the backmix model residence time with the conversion factor, R .



ERDA	_____
PAGE	_____
REVISION No.	_____
DATE	_____



**PRELIMINARY
FOR REVIEW ONLY**

Figure 9. CONVERSION FACTOR FOR PLUG-FLOW MODEL

C. FLUIDIZATION

1. Minimum Fluidization

The Kunii and Levenspiel¹⁰ correlation was found to be adequately descriptive of most of the published data on coal and related materials.⁷ Nevertheless, we recognize that a correlation that does not require information either of the particle shape factor or the incipient fluidized-bed voidage will be of greater practical utility.

Even though the published correlations by Leva,¹¹ Frantz,⁶ Wen and Yu,¹⁹ and several others belong to this class, they were shown to be in need of adjustment of coefficients to describe the published data within reasonable limits.⁷

Of the experimental data used to test the suitability of the published minimum fluidization velocity correlations, the data by Leva et al.¹³ and Jones et al.⁸ were excluded on the basis of the discussion presented earlier.⁷

To develop a correlation sufficiently descriptive of coal and related materials, the following form of the Kunii and Levenspiel correlation¹⁰ was chosen:

$$\frac{1.75}{\phi \cdot \epsilon_{mf}^3} (Re_{mf})^2 + \frac{150(1 - \epsilon_{mf})}{\phi^2 \cdot \epsilon_{mf}^3} \cdot Re_{mf} - Ga = 0 \quad (1)$$

where —

$$Re_{mf} = \frac{D_p \rho_g U_{mf}}{\mu} \quad (2)$$

= Reynolds number at minimum fluidization velocity

$$Ga = \frac{D_p^3 \rho_g (\rho_s - \rho_g) g}{\mu^2} \quad (3)$$

= Galileo number

ϕ = shape factor

ϵ_{mf} = voidage of minimum fluidized bed

Wen and Yu,¹⁹ in attempting to develop a correlation for minimum fluidization velocity, have assigned average values to the two groups, namely, $1/(\phi \cdot \epsilon_{mf}^3)$ and $(1 - \epsilon_{mf})/(\phi^2 \cdot \epsilon_{mf}^3)$, for the type of fluidization systems under investigation. In the present study, these two groups are treated as two parameters, and their values were determined by a nonlinear regression analysis of the Kunii and Levenspiel correlation,¹⁰ with the selected data on coal and related materials. As a result, the following empirical values were determined for the two parameters:

$$\frac{1}{\phi \cdot \epsilon_{mf}^3} = 8.81 \quad (4)$$

and

$$\frac{1 - \epsilon_{mf}}{\phi^2 \cdot \epsilon_{mf}^3} = 5.19 \quad (5)$$

Substituting these values in Equation 1 and simplifying the following correlation for U_{mf} can be obtained:

$$U_{mf} = \left(\frac{\mu}{\rho_g D_p} \right) \left\{ \left[(25.25)^2 + 0.0651 Ga \right]^{1/2} - 25.25 \right\} \quad (6)$$

A comparison of this correlation with the measured values of minimum fluidization velocity values is shown in Figure 10.

To evaluate the comparison of the calculated values with the measured values, the following quantity is defined:

$$\text{Standard Relative Deviation} = \left\{ \frac{\sum [(U_{mfC} - U_{mfM})/U_{mfM}]^2}{N - 2} \right\}^{1/2} \quad (7)$$

The standard relative deviation for the data shown in Figure 10 was determined for the proposed correlation, given by Equation 6, and the correlations tested for comparison.⁷ The percent standard relative deviations calculated for these correlations are shown in Table 1. It is apparent from this table that the proposed correlation provides a better estimate of the

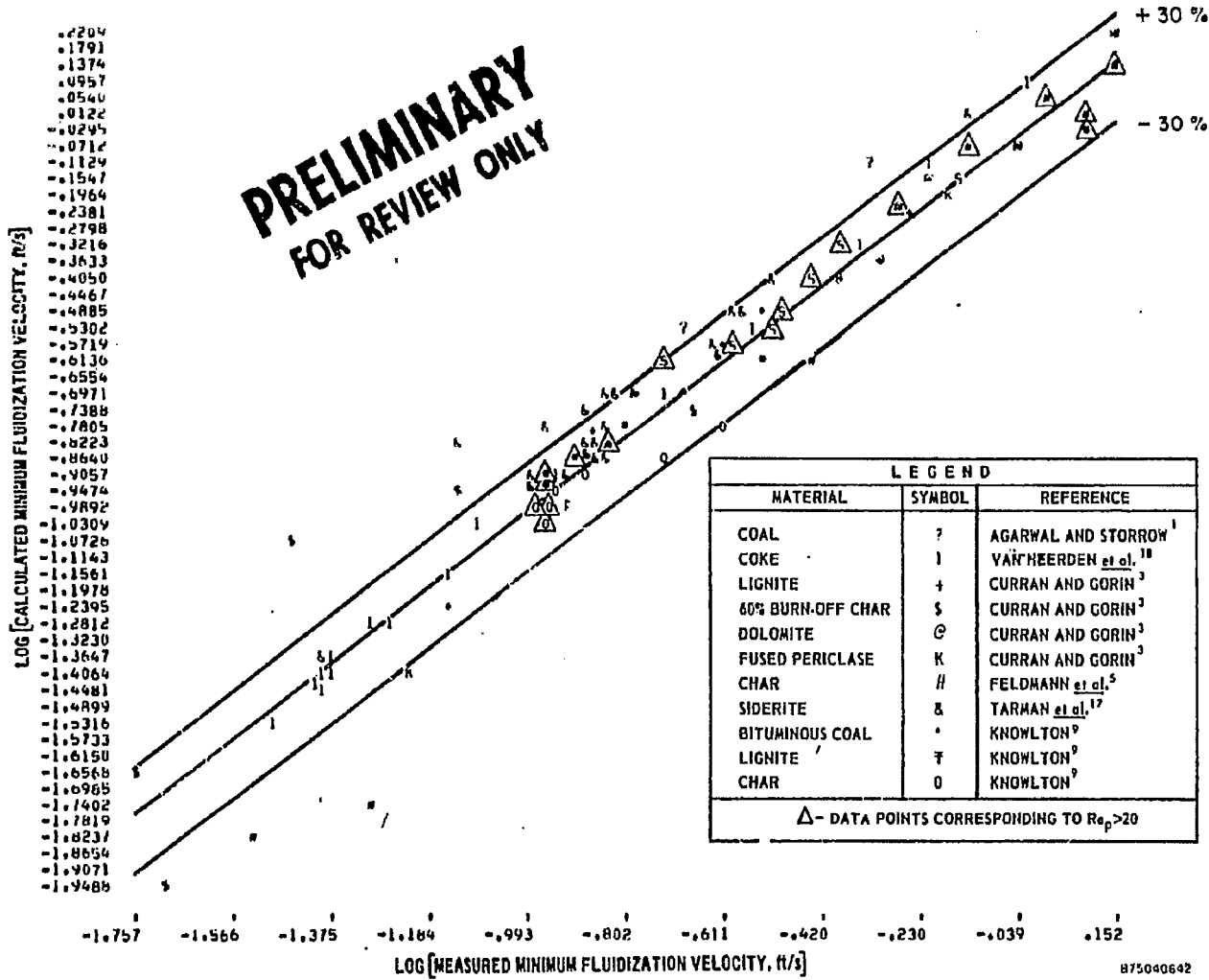


Figure 10. COMPARISON OF THE PROPOSED CORRELATION WITH MEASURED MINIMUM FLUIDIZATION DATA



ERDA	PAGE
DATE	REVISION No.

Table 1. SUMMARY OF ERROR ANALYSIS BETWEEN THE TESTED⁷ AND PROPOSED CORRELATION WITH MEASURED MINIMUM FLUIDIZATION VELOCITY

<u>Correlation</u>	<u>Standard Relative Deviation, %</u>
Frantz ⁶	52.46
Kunii-Levenspiel ¹⁰	50.63
Wen-Yu ¹⁹	47.27
Leva ¹¹	37.13
Zenz ²⁰	197.32
Proposed Correlation	29.09

minimum fluidization velocity, with $\pm 30\%$ standard relative deviation. This is supported by a comparison of Figure 10 with Figures 7 through 11 published in last month's report. Based on the above analysis, the proposed correlation is recommended for calculating minimum fluidization velocities for coal and related materials for pressures ranging from 1 to 70 atmospheres and for the entire range of particle Reynolds numbers.

2. Bed Expansion on Fluidization

The determination of fluidized-bed height at a given fluid velocity is important for the design and operation of fluidized beds. The fluidized-bed expansion characteristics are useful for the design of the transport disengagement section of the fluidized bed to estimate solids circulation rate, solids and fluid holdup, heat transfer from solids to fluid and walls of the container, mass-transfer between solids and fluid, and to predict the chemical kinetics and conversion in fluidized beds.

Several correlations were developed to estimate liquid fluidized-bed expansion characteristics, based on the assumption that liquid-solid fluidization is analogous to sedimentation.^{3, 14, 15} However, most of these correlations are generally applicable to narrow size range particles. The published expressions to predict fluidized-bed height as a function of gas velocity are few. Kunii and Levenspiel¹⁰ note that the poor agreement between the published data and the bed-expansion correlations is caused by the difficulty in measuring heights of a violently fluctuating surface of the bed.

a. Gas-Solid Fluidized Beds

From the hydrodynamics of fluidized beds, it is apparent that the bed expansion is related in a complex manner to the physical properties of solids and fluids, the gas flow in excess of the minimum fluidization velocity, the size and velocity of gas bubbles in aggregative fluidization, the bed height to diameter ratio, etc. Superimposed on this complicated relationship is the nonuniform bed density in a fluidized bed as identified by the three distinct zones, namely, a distributor effect zone, a zone of constant bed density, followed by a zone of continuously decreasing bed density,² which makes it difficult to estimate fluidized-bed heights.

A summary of the available methods to predict fluidized-bed expansions is given in Table 2. The published data on coal and related materials used to test the suitability of the bed-expansion correlations are given in Table 3.

b. Applicability of Proposed Correlations

The simplicity of the bed-expansion expression for particulate fluidization, developed by assuming a similarity to sedimentation, is very attractive for fluidization calculations. The suitability of this correlation to gas-solid fluidized beds, in particular for coal and related materials, was verified as follows.

The relationship between the fluid velocity (U), the corresponding bed expansion described by bed voidage (ϵ), and the terminal velocity of particles (U_t) is given by —

$$\epsilon = \left(\frac{U}{U_t} \right)^{1/n} \quad (8)$$

where n is related to the particle properties and the fluidization system.⁴

Using published data, n was determined by —

$$n = \frac{-\log U_t / U_{mf}}{\log \epsilon_{mf}} \quad (9)$$

Table 2. SOME PUBLISHED CORRELATIONS TO PREDICT FLUIDIZED-BED EXPANSION

Investigator	Bed Diameter, inches	Fluidized Solids	Fluidizing Medium	Proposed Correlation
Leva <u>et al.</u> ¹²	2.5 and 4	Sand	Air, CO ₂	$\frac{L_f}{L_{mf}} = \frac{U_{mf}}{U} \left[\frac{(1 - \epsilon)^2 \epsilon_{mf}^3}{(1 - \epsilon_{mf})^2 \epsilon^3} \right]^m$
Lewis <u>et al.</u> ¹⁴	2.5 and 4.5	Scotchlike glass beads	Air, water	$\frac{L_f}{L_{mf}} = 1 - \frac{0.0187 (U - U_{mf})}{D_p^{0.5}}$
Richardson and Zaki ¹⁵	2.44	Ballotini, ball bearings, glass spheres, lead shot, divinyl benzene	Water, glycerol-water, oil	$\frac{U}{U_t} = (\epsilon)^n$ <p>For very small D_p / D_T values:</p> $n = 4.65 \quad Re_t < 0.2$ $n = 4.40 (Re_t)^{-0.03} \quad 0.2 < Re_t < 1$ $n = 4.40 (Re_t)^{-0.1} \quad 1 < Re_t < 500$ $n = 2.40 \quad Re_t > 500$
Shen and Johnstone ¹⁶	--	--	--	$\frac{L_f}{L_{mf}} = 1 + \frac{0.0188 (U - U_{mf})}{D_p^{0.5}}$
Bakker and Heertjes ²	3.54	Glass beads	Air	Based on two-phase theory and bubble characteristics

Table 3. SOURCES OF FLUIDIZED-BED EXPANSION DATA FOR COALS AND RELATED MATERIALS (at 70° to 80°F)

<u>Investigators</u>	<u>Bed Diameter, inches</u>	<u>Fluidized Solids</u>	<u>Particle Diameter, inches</u>	<u>Particle Density, lb/cu ft</u>	<u>Fluidizing Medium</u>	<u>Operating Pressure, psig</u>	<u>Range of U/U_{mf}</u>	<u>Range of L_f/L_{mf}</u>
Curran and Gorin ³	1 and 2	Lignite char, dolomite, periclase	0.0028-0.0173	51-222	N ₂ , H ₂ , CO ₂	0	1-20.5	1-2
Feldmann et al. ⁵	3.69	Char	0.0052	23	CO ₂	0	1-12.0	1-1.53
Tarman et al. ¹⁷	2.5		0.00269 0.0141	245	Air, Freon	40.0	1-9.75	1-1.49

and the bed expansion as a function of gas velocity was calculated from Equation 8. The bed height (L_f) at any gas velocity (U) is related to the minimum fluidizing conditions (L_{mf} and ϵ_{mf}) in the following manner:

$$\frac{L_f}{L_{mf}} = \frac{1 - \epsilon_{mf}}{1 - (U/U_t)^{1/n}} \quad (10)$$

A comparison of the measured bed expansion with the calculated value from Equation 10 is shown in Figure 11. It is apparent that the agreement between the correlation and the data is very poor. Hence, it can be concluded that this simple model is not descriptive of the fluidization characteristics of coal and related materials.

As an alternative procedure, the values assigned by Richardson and Zaki¹⁵ to the exponent, n , for different regions of Reynolds numbers, ($Re_t = U_t \cdot D_p \cdot \rho_g / \mu$), were used to calculate bed expansion from Equation 10.

The calculated bed-expansion values using these values and Equation 3 are compared with the measured values in Figure 12. No improvement in comparison between the measured and calculated values is observed in Figure 12 as well, which indicates the nonsuitability of these correlations to describe the aggregative fluidization of coal and related materials.

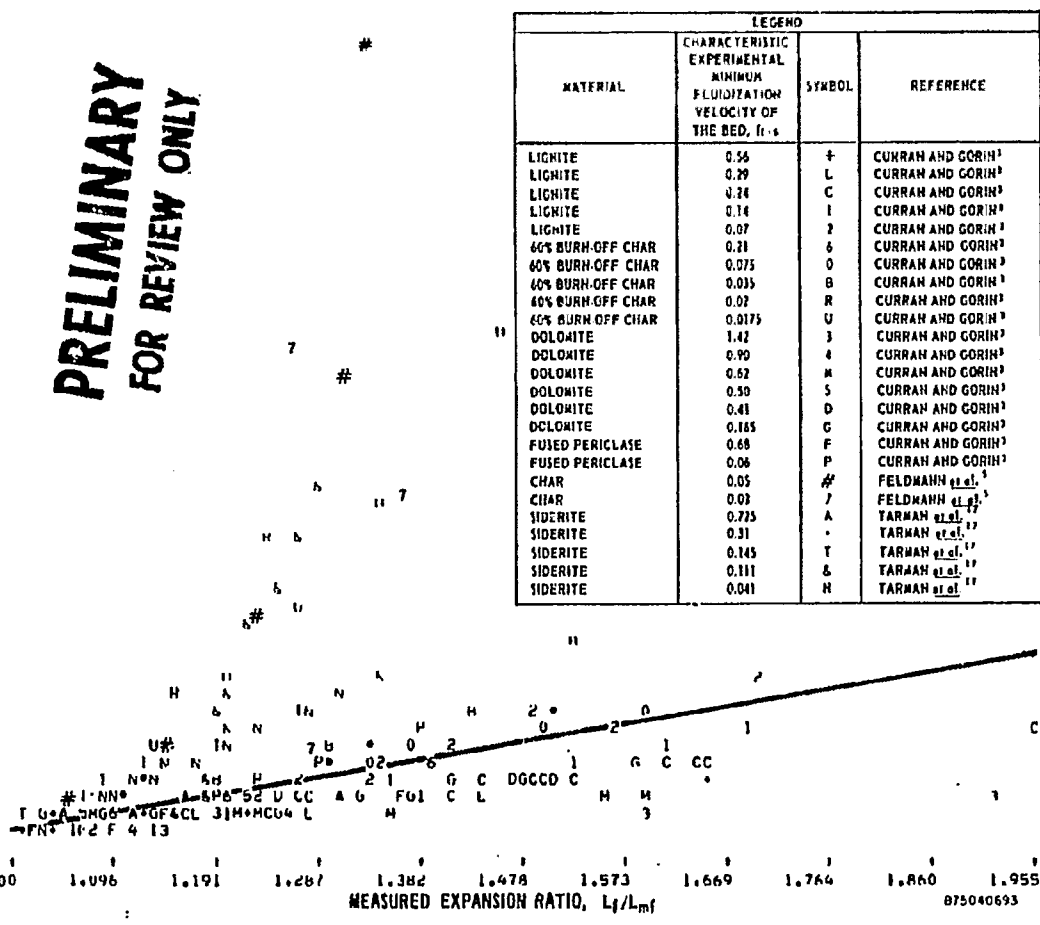
Work is in progress to test the comparisons of the other published correlations shown in Table 2 with the measured fluidized-bed expansion data.

3. Nomenclature

- D_f = particle diameter of a sieved fraction, ft
 D_p = average particle diameter, ft = $\frac{1}{\Sigma(X/D_f)}$
 D_T = tube diameter, ft
 Ga = Galileo number
 g = gravitational constant, ft/s²

5.8723
 5.7785
 5.6847
 5.5909
 5.4971
 5.4034
 5.3096
 5.2158
 5.1220
 5.0283
 4.9345
 4.8407
 4.7469
 4.6532
 4.5594
 4.4656
 4.3718
 4.2781
 4.1843
 4.0905
 3.9967
 3.9030
 3.8092
 3.7154
 3.6216
 3.5279
 3.4341
 3.3403
 3.2465
 3.1528
 3.0590
 2.9652
 2.8714
 2.7777
 2.6839
 2.5901
 2.4963
 2.4026
 2.3088
 2.2150
 2.1212
 2.0274
 1.9337
 1.8399
 1.7461
 1.6523
 1.5586
 1.4648
 1.3710
 1.2772
 1.1835
 1.0897
 .9959

**PRELIMINARY
 FOR REVIEW ONLY**



ERDA _____

PAGE _____

REVISION No. _____

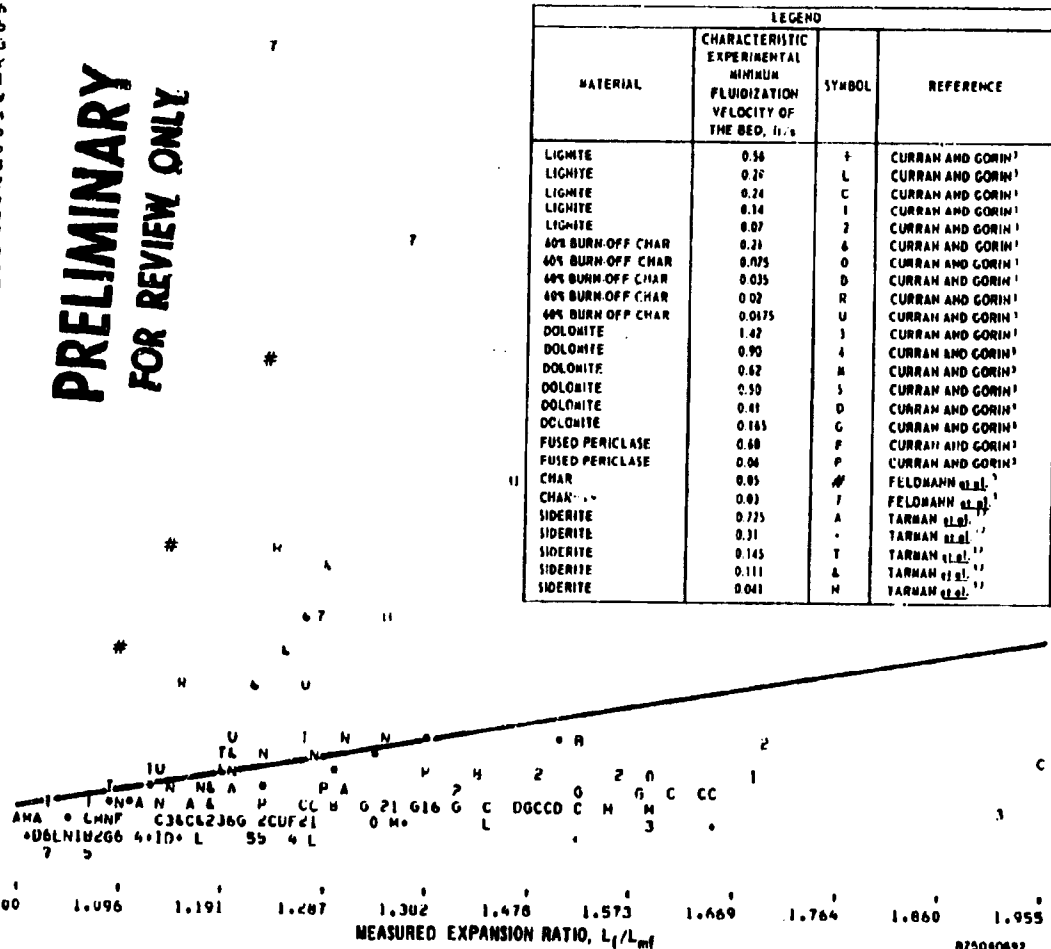
DATE _____

Figure 11. COMPARISON OF CALCULATED VALUES FROM EQUATION 10 WITH THE MEASURED FLUIDIZED-BED EXPANSION DATA

CALCULATED EXPANSION RATIO, L_f/L_{mf}

5.6671
 5.5714
 5.4768
 5.3816
 5.2865
 5.1913
 5.0962
 5.0011
 4.9059
 4.8108
 4.7156
 4.6205
 4.5253
 4.4302
 4.3350
 4.2399
 4.1447
 4.0496
 3.9544
 3.8593
 3.7641
 3.6690
 3.5738
 3.4787
 3.3835
 3.2884
 3.1932
 3.0981
 3.0029
 2.9078
 2.8126
 2.7175
 2.6223
 2.5272
 2.4321
 2.3369
 2.2418
 2.1466
 2.0515
 1.9563
 1.8612
 1.7660
 1.6709
 1.5757
 1.4806
 1.3854
 1.2903
 1.1951
 1.1000
 1.0048
 0.9097
 0.8145
 0.7194

**PRELIMINARY
FOR REVIEW ONLY**



LEGEND			
MATERIAL	CHARACTERISTIC EXPERIMENTAL MINIMUM FLUIDIZATION VELOCITY OF THE BED, ft/s	SYMBOL	REFERENCE
LIGNITE	0.56	F	CURRAN AND GORIN ¹
LIGNITE	0.76	L	CURRAN AND GORIN ¹
LIGNITE	0.74	C	CURRAN AND GORIN ¹
LIGNITE	0.14	I	CURRAN AND GORIN ¹
LIGNITE	0.87	Z	CURRAN AND GORIN ¹
40% BURN-OFF CHAR	0.71	A	CURRAN AND GORIN ¹
40% BURN-OFF CHAR	0.875	O	CURRAN AND GORIN ¹
40% BURN-OFF CHAR	0.035	D	CURRAN AND GORIN ¹
40% BURN-OFF CHAR	0.02	R	CURRAN AND GORIN ¹
40% BURN-OFF CHAR	0.0175	U	CURRAN AND GORIN ¹
DOLOMITE	1.42	J	CURRAN AND GORIN ¹
DOLOMITE	0.90	A	CURRAN AND GORIN ¹
DOLOMITE	0.62	M	CURRAN AND GORIN ¹
DOLOMITE	0.50	S	CURRAN AND GORIN ¹
DOLOMITE	0.41	D	CURRAN AND GORIN ¹
DOLOMITE	0.165	G	CURRAN AND GORIN ¹
FUSED PERICLASE	0.68	F	CURRAN AND GORIN ¹
FUSED PERICLASE	0.04	P	CURRAN AND GORIN ¹
CHAR	0.65	H	FELDMANN et al. ²
CHAR	0.63	I	FELDMANN et al. ²
SIDERITE	0.775	A	TARHAN et al. ³
SIDERITE	0.31	-	TARHAN et al. ³
SIDERITE	0.145	T	TARHAN et al. ³
SIDERITE	0.111	A	TARHAN et al. ³
SIDERITE	0.041	N	TARHAN et al. ³



ERDA _____
 PAGE _____
 REVISION No. _____
 DATE _____

Figure 12. COMPARISON OF CALCULATED VALUES FROM EQUATION 9 WITH ASSIGNED VALUES FOR n^{15} WITH THE MEASURED FLUIDIZED-BED EXPANSION DATA

875040892

L_{mf}	=	height of minimum fluidized bed
L_f	=	height of fluidized bed
m	=	constant
n	=	constant
N	=	number of data points
Re_t	=	particle Reynolds number $(D_p \cdot U_t \cdot \rho_g / \mu)$
Re_{mf}	=	particle Reynolds number $= (D_p \cdot U_{mf} \cdot \rho_g / \mu)$
U	=	superficial gas velocity, ft/s
U_{mf}	=	minimum fluidization velocity, ft/s
U_{mfC}	=	calculated minimum fluidization velocity, ft/s
U_{mfM}	=	measured minimum fluidization velocity, ft/s
U_t	=	terminal velocity, ft/s
X	=	weight fraction of sieved particles
ϵ	=	fractional volume occupied by bubbles and voids in a fluidized bed
ϵ_{mf}	=	voidage of minimum fluidized bed
ϕ	=	shape factor
ρ_g	=	density of fluidizing gas, lb/CF
ρ_s	=	particle density of fluidizing solids, lb/cu ft
μ	=	viscosity of fluidizing gas, lb/ft-s

4. References Cited

1. Agarwal, O. P. and Storrow, J. A., "Pressure Drop in Fluidized Beds - Part I," Chem. Ind. (London), 278-86 (1951) April 14.
2. Bakker, P. J. and Heertjes, P. M., "Porosity Distributions in a Fluidized Bed," Chem. Eng. Sci. 12, 260 (1960).
3. Curran, G. P. and Gorin, E., "Studies on Mechanics of Fluo-Solids Systems," prepared for Office of Coal Research, Contract No. 14-01-0001-415, Interim Report No. 8, Book 1. Washington, D. C., 1970.

4. Davidson, J. F. and Harrison D., Fluidized Particles London: Cambridge Univ. Press, 1963.
5. Feldmann, H. F., Kiang, K. and Yavorsky, P., "Fluidization Properties of Coal Char," Symposium on Gasification of Coal, 162nd National Meeting, ACS Division of Fuel Chemistry Preprints 15, (3), 62-76 (1971) September.
6. Frantz, J. F., "Minimum Fluidization Velocities and Pressure Drop in Fluidized Beds," Chem. Eng. Progr. Symp. Ser. 62, 21-31 (1966).
7. Institute of Gas Technology, "Preparation of a Coal Conversion Systems Technical Data Book," ERDA Contract No. 14-32-0001-1730, Rep. No. 4. Chicago, February 1975.
8. Jones, J. F., Eddinger, R. T. and Seglin, L., "Pyrolysis of Agglomerating Coals in Multiple Fluidized-Bed Reactors," in Proceedings of the International Symposium on Fluidization, Amsterdam: Netherlands Univ. Press, 1967.
9. Knowlton, T. M., "High-Pressure Fluidization Characteristics of Several Particulate Solids: Primarily Coal and Coal-Derived Materials." Paper No. 9b, presented at the 67th Annual Meeting of the A. I. Ch. E., Washington, D. C., December 1-5, 1974.
10. Kunii, D. and Levenspiel, O., Fluidization Engineering. New York: John Wiley, 1969.
11. Leva, M., Fluidization. New York: McGraw-Hill, 1959.
12. Leva, M., Grummer, M., Weintraub, M. and Pollichik, M., "Fluidization of Solid Non-Vesicular Particles," Chem. Eng. Progr. 44, 619 (1948).
14. Leva, M., Weintraub, M., Grummer, M. and Pollichik, M., "Fluidization of an Anthracite Coal," Ind. Eng. Chem. 41, 1206 (1949).
15. Richardson, F. F. and Zaki, W. N., "Sedimentation and Fluidization: Part I," Trans. Inst. Chem. Eng. 32, 35 (1954)
16. Shen, C. Y. and Johnstone, H. F., "Gas-Solid Contact in Fluidized Beds," A. I. Ch. E. J. 1, 349 (1955).
17. Tarman, P., Punwani, D., Bush, M. and Talwalkar, A., "Development of the Steam-Iron System for Production of Hydrogen for the HYGAS Process," prepared for Office of Coal Research, Contract No. 14-32-0001-1518, R&D Report No. 95, Interim Report No. 1. Washington, D. C., 1974.
18. van Heerden, C., Nobel, A. P. P. and van Krevelen, D. W., "Studies on Fluidization I - The Critical Mass Velocity," Chem. Eng. Sci. 1, No. 1, 37-49 (1951).

19. Wen, C. Y. and Yu, Y. H. "Mechanics of Fluidization," Chem. Eng. Progr. Symp. Ser. 62, 100-11 (1966).
20. Zenz, F. A., "Calculate Fluidization Rates," Pet. Refiner 36, No. 8, 147-55 (1957).

5. Errata

In last month's report (Project 8964 February 1975 Status Report), the following correction is to be noted:

In Table 3 (page 36), the particle density range for Curran and Gorin's data is 51-222 lb/cu ft instead of 51-122 lb/cu ft.

D. COMBUSTION

A mathematical model is being developed to describe the sulfur removal from the fluidized-bed combustors.

E. COAL, CHAR, AND OIL SHALE PROPERTIES

1. Coal Data Compilation

A table showing the location and size of coal deposits large enough to be considered as potential sites of conversion plants is being prepared. Its purpose is to aid in the selection of samples for our compilation of property data on selected coal samples. A county-seam entry appears adequate for states east of the Mississippi because counties there are generally small. In Western States, counties are often large enough to contain plants in more than one field or location, so entry by coal field will be necessary. Entry by seam is necessary because sampling is usually done on this basis.

As a criterion for inclusion of deposits in this table, we have chosen, for underground mining, a reserve base of 300 million tons or more of coal; experts estimate that about half of such reserve-base amounts can actually be produced with current technology. For strip-mining, our criterion is 150 million tons or more of "strippable reserve," as defined by the Bureau of Mines, that is, an estimate of the amount that can actually be produced with current strip-mining technology. In those cases where reserves of both categories exist in the same country, both will be reported if one or the other meets the criterion.

The table has been completed for underground mining, based on data of a recently issued Bureau of Mines' publication.* Entries for strip-mining remain to be added. State geological survey publications are being consulted for the latter, as county-seam and coal field-seam information is not available from the Bureau of Mines' publications.

2. Specific Heat of Coal, Char, and Ash

Data on enthalpy and specific heat of coal and related materials were reviewed by McCabe and Boley in 1945 (Lowry),⁹ Clendenin and coworkers in 1949,⁴ Agroskin in 1959,¹ Badzioch in 1960,² Kirov in 1965,⁸ and Gomez and coworkers of the Bureau of Mines in 1965.⁶ The last study, including both original work and that of others, was limited to temperatures at which the coal does not decompose. Heat effects at higher temperatures have been included in other studies. The most ambitious of these is the work of Kirov⁸; he presents a correlation covering all ranks of coal and their devolatilization products at temperatures from 0° to 1100°C.

Kirov's correlation⁸ is based on consideration of the specific heat of coal as the summation of the specific heats, on a weight basis, of the components including moisture, low-temperature volatile matter, high-temperature volatile matter, ash-free coke, and ash.

Correlations are simplified by presentation on a moisture-free and ash-free basis. Volatile matter after volatilization is considered to be entirely removed during subsequent temperature rises. Thus, enthalpies of pyrolysis are included, but not the sensible heat of the vaporous or gaseous products of pyrolysis.

Kirov's correlation,⁸ expressed as mean specific heat above 0°C per gram of raw coal, is shown in Figure 13. The values after onset of devolatilization are for complete devolatilization at the temperature in question, according to the correlation of Gregory and Littlejohn.⁷ Data used by Kirov for specific heats of ash and coke are shown in Figures 14 and 15, respectively. Data relating to the specific heat of volatile matter are shown in Figures 16 and 17.

* U. S. Bureau of Mines, "The Reserve Base of Bituminous Coal and Anthracite for Underground Mining in the Eastern United States," IC8655. Pittsburgh, 1974.

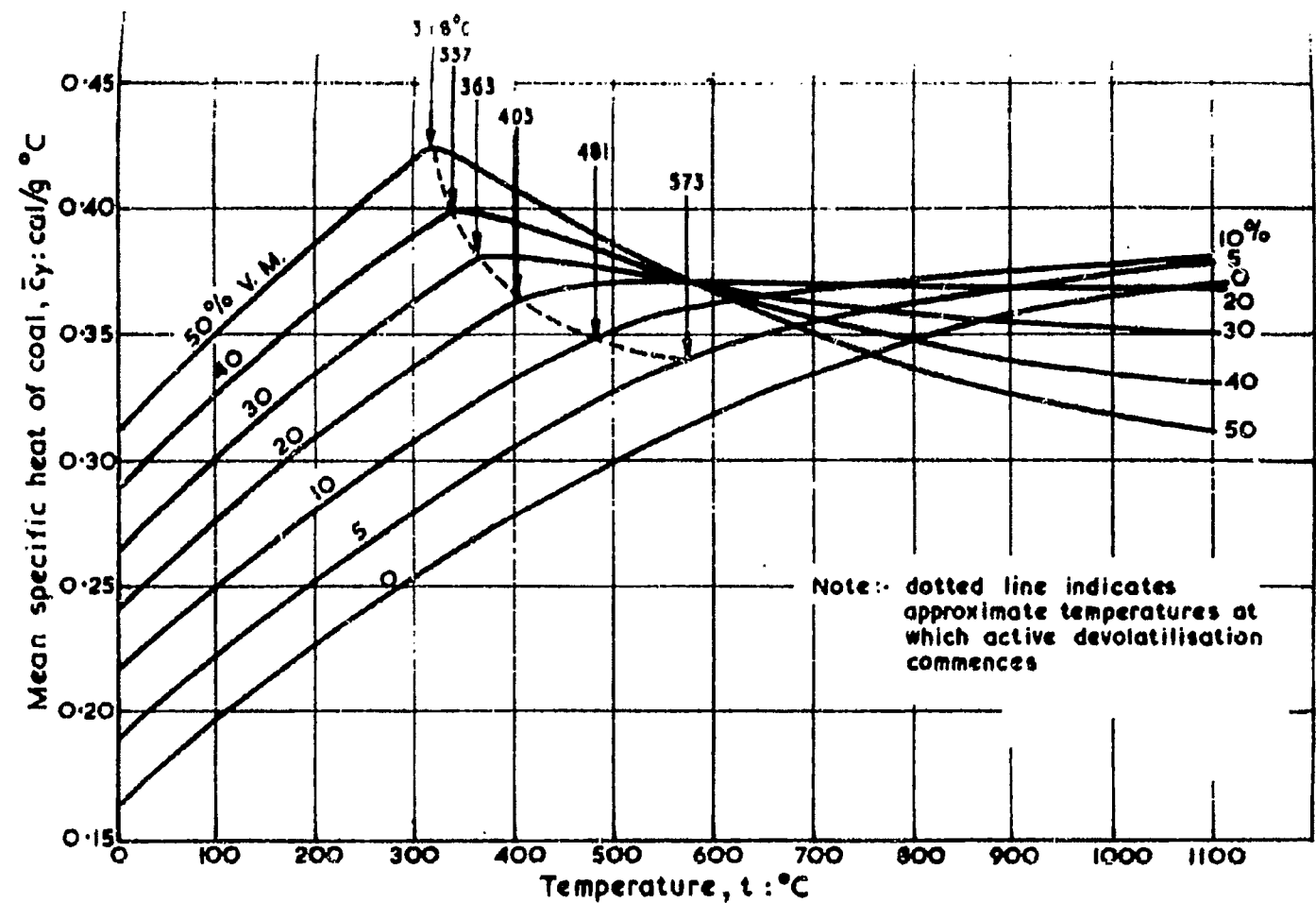


Figure 13. MEAN SPECIFIC HEATS OF COAL RESIDUES AT ELEVATED TEMPERATURES, EXPRESSED ON THE BASIS OF 1 GRAM OF RAW COAL (d. a. f.)⁸

3/75

8964

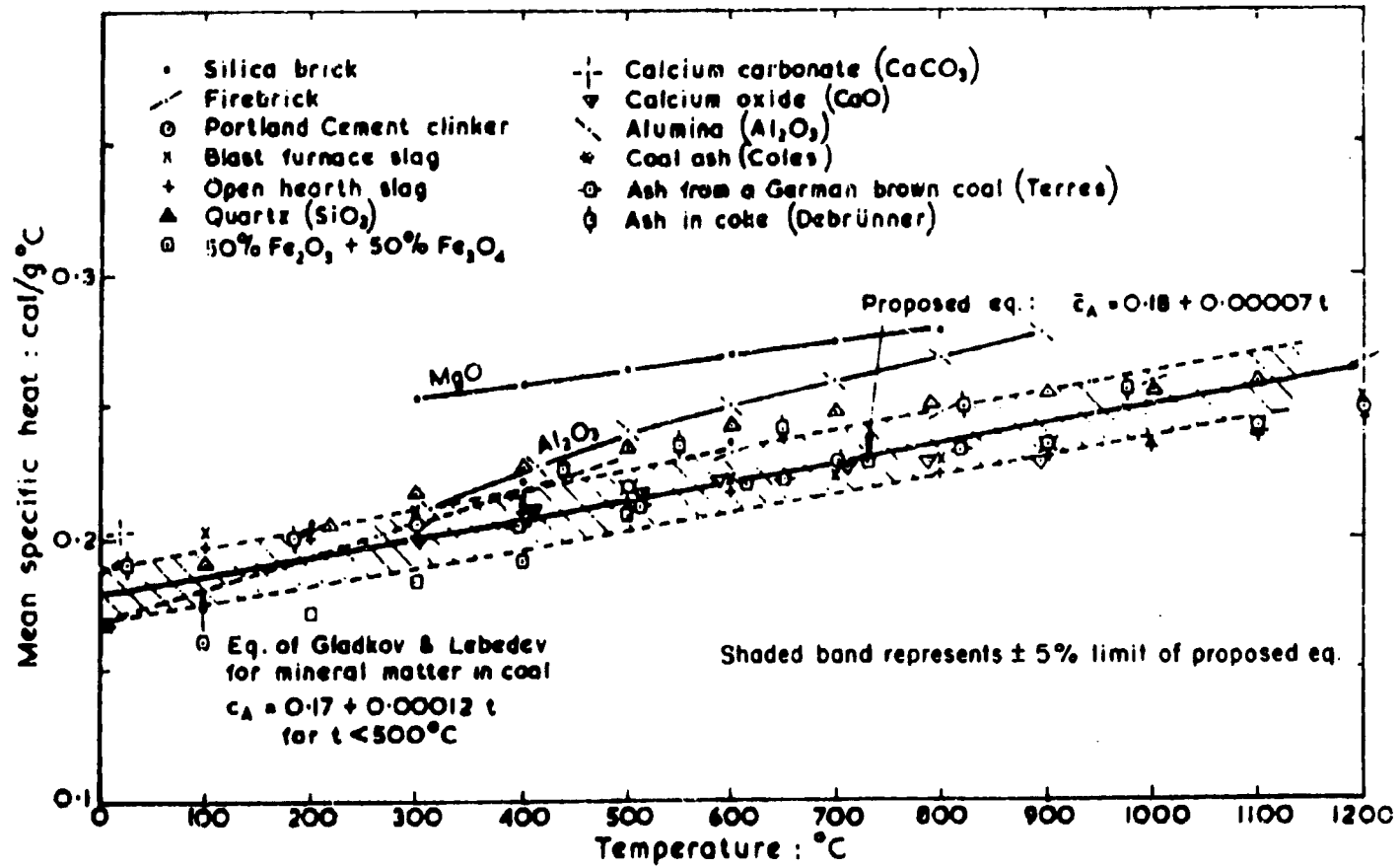


Figure 14. MEAN SPECIFIC HEATS OF ASH, SLAG AND CLINKER, AND OF THEIR MAIN CONSTITUENTS⁸

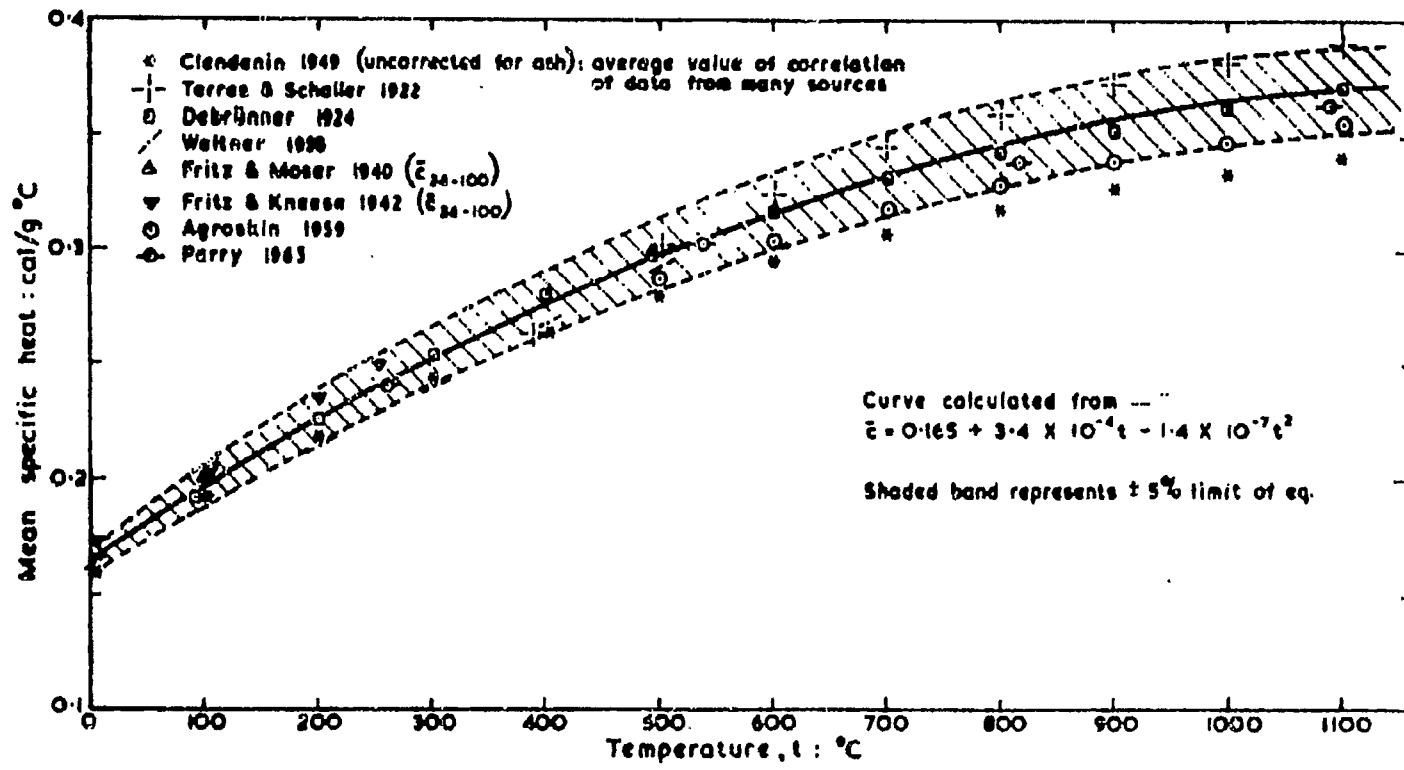


Figure 15. MEAN SPECIFIC HEATS OF HIGH-TEMPERATURE COKES⁸

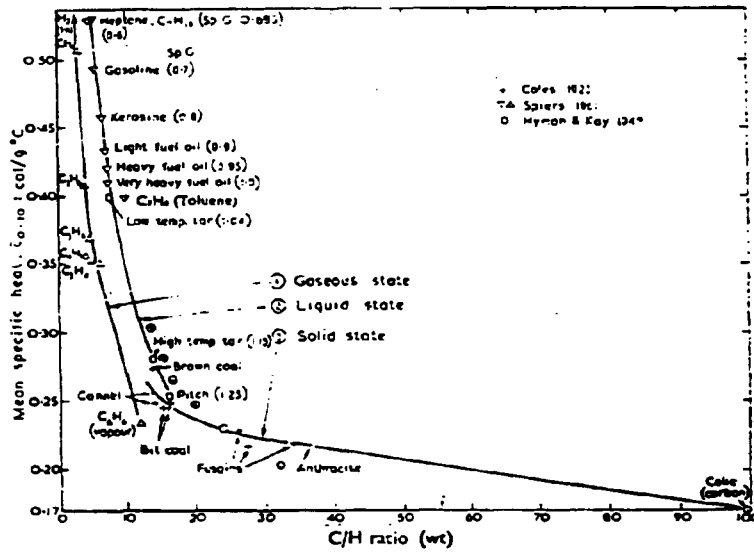


Figure 16. RELATION BETWEEN SPECIFIC HEATS AND CARBON/HYDROGEN RATIO OF HYDROCARBON AND COALS⁸

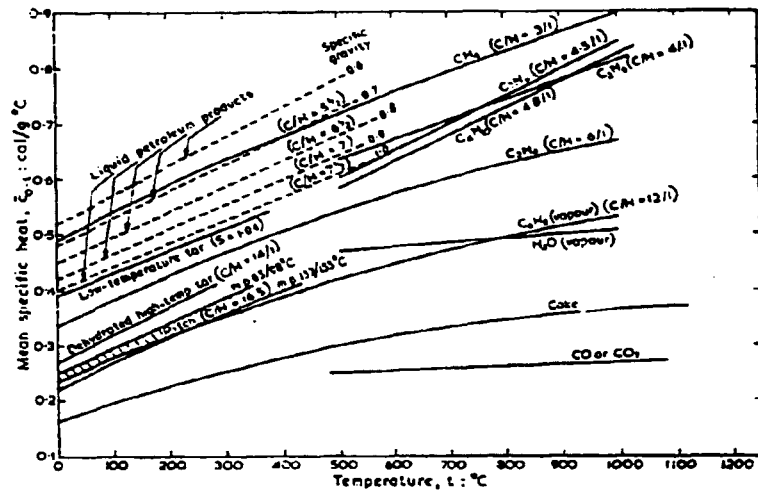


Figure 17. SPECIFIC HEAT-TEMPERATURE RELATIONS FOR LIQUID AND GASEOUS HYDROCARBONS⁸

The combination of experimental specific heats of anthracite with those of cokes yielded specific heats of the volatile matter in anthracite (and low-volatile chars) according to the following equation:

$$C_{V2}, \text{ cal/g-}^\circ\text{C} = 0.71 + 6.1 \times 10^{-4}t$$

These values are within the range of those for methane and hydrogen-rich volatile matter released by such samples at high temperatures (Figure 16). The specific heat of volatile matter present in excess of 10% was estimated from the equation of Cragoe⁵ for a low-temperature tar of specific gravity 1.04 in the condensed (liquid) phase:

$$C_{V1}, \text{ cal/g-}^\circ\text{C} = 0.395 + 8.1 \times 10^{-4}t$$

These two equations are for instantaneous specific heats; mean values are obtained if the temperature coefficients are reduced by one-half. A comparison of the correlation with experimental values is shown in Figure 18.

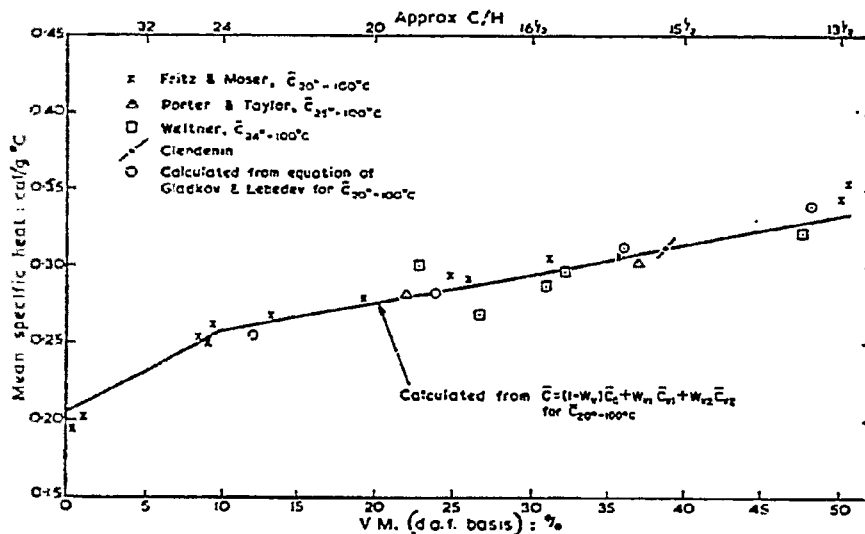


Figure 18. THE INFLUENCE OF VOLATILE MATTER (Rank and Petrological Composition) ON THE MEAN SPECIFIC HEATS OF RAW COALS⁸

We are critically reviewing specific heat data with the view to adopting Kirov's approach. Thermochemical data on mineral matter components, in contradistinction to ash components, and on mineral intermediate conversion products are being reviewed, with results to date shown in Figure 19. We think that conclusions based on these types of data should be confirmed by enthalpy determinations on samples obtained by the recently developed techniques of low-temperature ashing. This is of greater importance for residues from conversion processes than for coal itself.

We also propose to check Kirov's correlation against experimental data including those obtained since his review. The literature has been searched, and most of the recent papers on the subject have been obtained.

3. References Cited

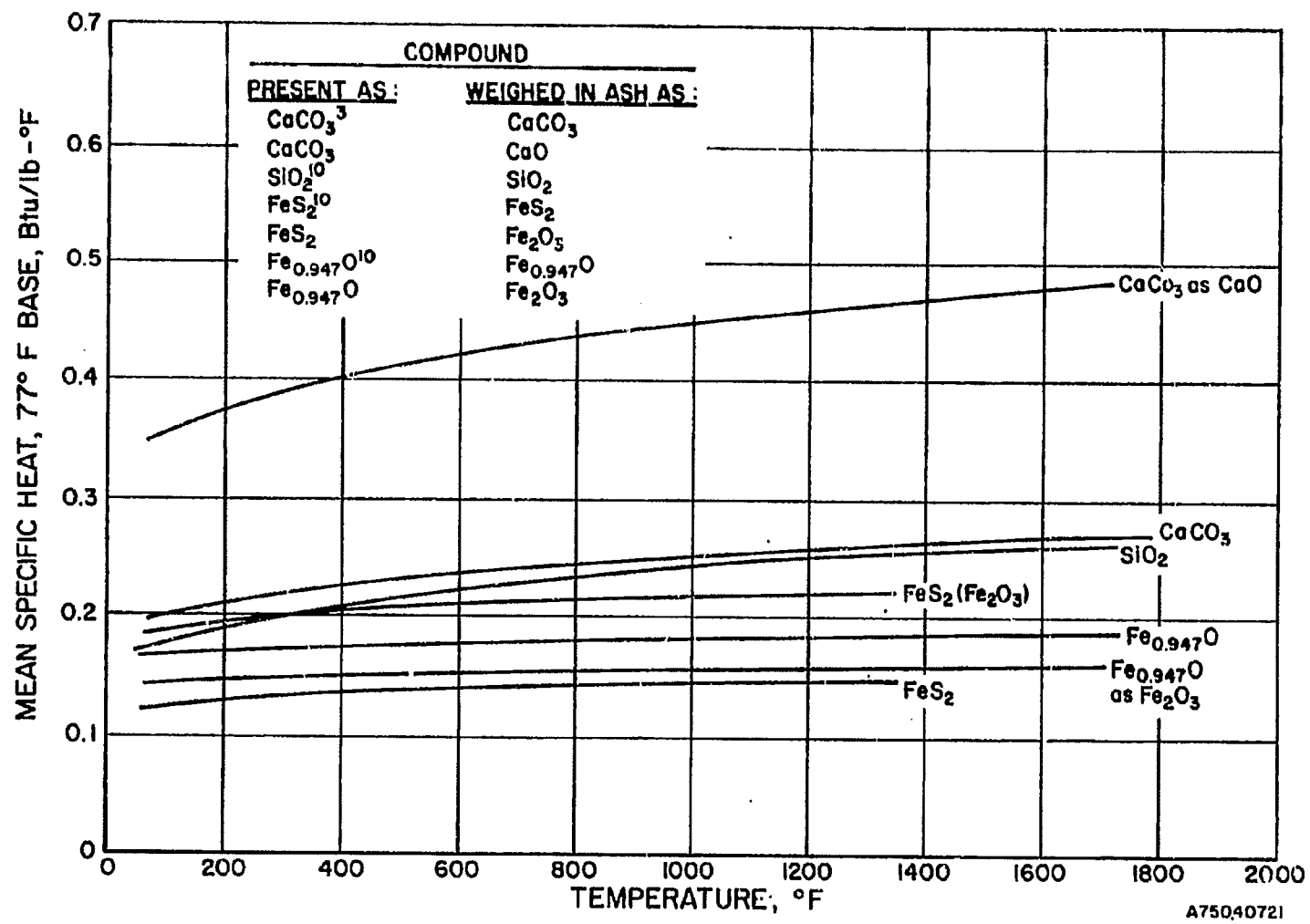
1. Agroskin, A. A., Thermal and Electrical Properties of Coal, Moscow: Gos. Nauch. Tekhn. Izd. Lit. Chern. Tsvetz. Metal., 1959 (Russian text).
2. Badzioch, S., "Thermo-Physical Properties of Coals and Cokes," Br. Coal Util. Res. Assoc. Mon. Bull. 24, 485-520 (1960) October-November.
3. Barin, I. and Knacke, O., Thermochemical Properties of Inorganic Substances. New York: Heidelberg, 1973.
4. Clendenin, J. D. et al., "Thermal and Electrical Properties of Anthracite and Bituminous Coals," Technical Paper 160, State College, Pa.: School of Mineral Mines, 1949.
5. Cragoe, C. S., "Thermal Properties of Petroleum Products," Misc. Pub. No. 97, Washington, D. C.: U. S. Bureau of Standards, 1929.
6. Gomez, M., Gayle, J. B. and Taylor, A. R., Jr., "Heat Content and Specific Heat of Coals and Related Products." U. S. Bur. Mines Rep. Invest. No. 6607. Pittsburgh, 1965.
7. Gregory, D. R. and Littlejohn, R. F., "A Survey of Numerical Data on the Thermal Decomposition of Coal," Br. Coal Util. Res. Assoc. Mon. Bull. 29, 173-80 (1965) June.
8. Kirov, N. Y., "Specific Heats and Total Heat Contents of Coals and Related Materials at Elevated Temperatures," Br. Coal Util. Res. Assoc. Mon. Bull. 29, 33-57 (1965) February-March.

PRELIMINARY FOR REVIEW ONLY

INSTITUTE OF GAS TECHNOLOGY

40

3/75



ERDA			
PAGE			
REVISION No.			
DATE			

Figure 19. MEAN SPECIFIC HEAT OF MINERAL COMPONENTS OF COAL AND CHAR

8964

9. McCabe, L. C. and Boley, C. C., "Physical Properties of Coals," in Lowry, H. H., Ed., Chemistry of Coal Utilization, Vol. I, 310-36. New York: John Wiley, 1945.
10. Stull, D. R. and Prophet, H., Eds., JANAF Thermochemical Tables, 2nd Ed. Washington, D. C.: U. S. Department of Commerce, National Bureau of Standards, June 1971.

IV. Patent Status

The work performed during March is not considered patentable.

V. Future Work

We plan to contact some of the experts in the liquefaction area referred to us by the Pittsburgh Energy Center of the U. S. Bureau of Mines.

We will continue to work in the selected five high-priority areas.

Approved

W. W. Bodle

W. W. Bodle, Director
Process Analysis

Signed

A. Talwalkar

A. Talwalkar, Coordinator,
Process Data

IGT-MPR--6

INSTITUTE OF GAS TECHNOLOGY



3424 SOUTH STATE STREET

IIT CENTER

CHICAGO, ILLINOIS 60616

AFFILIATED WITH ILLINOIS INSTITUTE OF TECHNOLOGY